FIRST OPERATION OF THE ELECTRO OPTICAL SAMPLING DIAGNOSTICS OF THE FERMI@ELETTRA FEL

M. Veronese*, A. Abrami, E. Allaria, M. Bossi, M.B. Danailov, M. Ferianis,
L. Fröhlich, S. Grulja, M. Predonzani, F. Rossi, G. Scalamera, C. Spezzani, M. Tudor, M. Trovò
Sincrotrone Trieste S.C.p.A., Trieste, Italy

Abstract

The FERMI@Elettra seeded FEL has demanding specifications in terms of longitudinal properties of the electron beam. Several diagnostics are installed along the linac. At the entrance of the FEL1 undulator chain an electro optical sampling (EOS) station based on the spatial encoding scheme is installed. The EOS provides both time jitter and longitudinal profile measurements in a non-destructive way. The layout of this system is described and the first operational measurement results obtained are reported. The paper includes also the capability of this diagnostics to perform the temporal coarse alignment of the seed laser to the electron beam. Finally a discussion on the future developments foreseen for this system is given.

INTRODUCTION

FERMI@Elettra is a seeded FEL operating in the spectral range from VUV to soft x-rays. It is based on a SLAC/BLN/UCLA type RF-gun and a normal conducting LINAC, currently operated at 1.2 GeV, but designed to reach 1.5 GeV. The longitudinal compression is provided by two magnetic chicanes BC1 and BC2 (respectively at 300 MeV and 600 MeV). The FEL has two undulator chains, namely FEL1 and FEL2. The first, FEL1, is a single cascade HGHG seed system designed to provide hundreds of microjoule per pulse in the wavelength range from 100 to 20 nm. The second, FEL2, is a double cascade seeded system designed to reach 4 nm as the shortest wavelength. A deep knowledge of the longitudinal parameters such as: longitudinal charge distribution, time of arrival jitter, slice energy spread and slice emittance is needed. For this reason FERMI@Elettra has been equipped with several longitudinal diagnostics to provide the necessary information for the commissioning and operation of the accelerator. They are: the Cherenkov low energy profile measurement with a femtosecond streak Camera, the Coherent Bunch Length Monitors (CBLM), the Bunch Arrival Monitors (BAM), the RF-deflecting cavities at low energy (LERFD) and at high energy (HERFDs) and finally the Electro Optical sampling stations (EOS). In this paper we present the layout and the first operational results from the EOS installed at the entrance of the FEL1 chain of FERMI. The Electro Optical Sampling provides single shot non-destructive longitudinal profile and time jitter measurements. For this reason it is installed just before the modulator undulator. In this position the EOS system provides also the coarse temporal alignment of the seed laser to the electron beam. In general an electro optical sampling diagnostics, makes use of the very large transient electric coulomb field of ultra-relativistic electron bunches to map their longitudinal profile. The electric field induces a variation in the crystal structure of an electro optic crystal. The refractive index variation is detected by optical polarization analysis. Since this effect is very fast, it reproduces the longitudinal distribution of the electron bunch with high fidelity. An ultrafast laser with pulse duration on the scale of 100 fs is an optimal probe. Several single shot schemes have been introduced and have been shown to be very effective (e.g. [1, 2]). For the FERMI FEL1 EOS we have chosen the spatial encoding scheme [3, 4]. This scheme is capable of providing high resolution measurements with the energy per pulse delivered by a compact, commercial, fiber laser oscillator.

For ultra-relativistic electrons the electric coulomb field has a large transverse component. For a single electron the electric field distance b from electron bunch in the plane (x,y) orthogonal the propagation direction (z) is [5]:

$$E_{y=b} = \frac{e}{4\pi\epsilon_0}\frac{\gamma b}{(b^2+\gamma^2 z^2)^{3/2}} \quad (1)$$

For an electron bunch with N_e electrons, the longitudinal distribution normalized to the maximum current, $\rho(z)$, can be approximated for the FERMI case to a rectangular distribution that is conveniently modeled by the difference of two Heaviside functions: $\rho(z) = H(z+FW\cdot/2) - H(z-FW\cdot/2)$. Then the total field along the axis is then:

$$E_{beam} = \int \rho(z-z')E_{0,b,z'}dz' \quad (2)$$

From Eq. 1 above , it is clear that the minimum distance between electron beam and EO crystal is a critical parameter and its proper selection depends on several factors. Very small distances are desirable, but this would induce wake-fields on the electron beam. Trajectory fluctuations may cause the e-beam to hit the EO crystal, possibly damaging it and producing ionizing radiation dose on the downstream undulators. Finally, in the EOS area, the seed laser travels collinearly to the electron beam, focusing from its entrance point upstream the EOS to reach it minimum width at the center of the modulator downstream the EOS. The seed laser has a high energy per pulse (up to tens of microjoules at a wavelength of 260 nm) that could potentially damage the crystal in case of an accidental impact. In practice, we should set the distance b at minimum to 5 mm. For a 500

* marco.veronese@elettra.trieste.it

ISBN 978-3-95450-119-9

pC electron bunch with a bunch length FWHM of around 1 ps, we get tens of MV/m of peak electric field. To evaluate the amplitude of the EO effect we consider the case of a laser pulse probing a crystal with zinc-blende crystal structure like ZnTe or GaP, cut along the normal to the (110) plane and a detection based on the balanced detector scheme. The EO signal is proportional to $\sin(\Gamma)$ where Γ is the phase retardation induced by the electric field of the electron beam as per Equation 3.

$$\Gamma = \frac{\pi d}{\lambda_0} n_0^3 E_{beam} r_{41} \sqrt{1 + 3\cos^2(\alpha)} \qquad (3)$$

Where d is the thickness of the crystal, λ_0 is the laser wavelength in vacuum, E_{beam} is the electric field due to the electron beam, r_{41} is the only independent element of electro-optic tensor for the chosen crystal structure, and finally α is the angle between the electric field of the electron bunch and the $[-1, 1, 0]$ direction. This translates for our laser and a crystal of $100\mu m$ thickness and $\alpha = 0$ to values for Γ of respectively: 0.3 for ZnTe and 0.8 for GaP, large enough to allow for single shot EO measurement.

LAYOUT

Figure 1 shows the layout of the EOS installed in the FEL1 line of FERMI@Elettra. The present setup is an evolution of the initial design [6]. It is based on a Menlosystems fiber laser, model TC780, installed in the accelerator tunnel, close to the EOS vacuum chamber, to minimize pointing and time stability issues that may be related to a long optical transport system. The laser is a frequency doubled 1560 nm femtosecond fiber laser, emitting at 780 nm, with a repetition rate of 78.895 MHz and an energy per pulse of 0.8 nJ with a pulse duration of 110 fs FWHM. The laser is phase locked to a pulsed optical phase reference distributed in one stabilized fiber link of the timing system [7]. A dedicated electronics converts optical pulses to RF and extracts a 1.499 GHz phase reference which is used by the phase locking electronics. The coarse time alignment is provided by phase shifting the 1.499 GHz reference with a vector modulator while keeping the laser locked, thus producing an effective delay of the exit time of the pulse from the laser. The fine temporal alignment is provided by a 200 mm travel delay line. A remotely controlled polarizer and a zero order $\lambda/2$ wave plate allow for adjustment of the input polarization. Before entering the vacuum chamber, the laser beam passes through a cylindrical lens that focus it in only one direction onto the EO crystals. The vacuum chamber is equipped with a 3 axis high precision manipulator currently equipped with: an OTR screen (a $1\mu m$ aluminum foil), used for coarse time alignment, a YAG:Ce crystal, for beam size measurement, two electro optic crystals and a calibration target. For the initial commissioning of the system the setup has been optimized for signal to noise ratio rather than for maximum resolution. Thus we installed a 1 mm thick ZnTe crystal and a GaP 0.4mm thick crystal. Figure 2 shows a detailed view of the in vacuum crystals

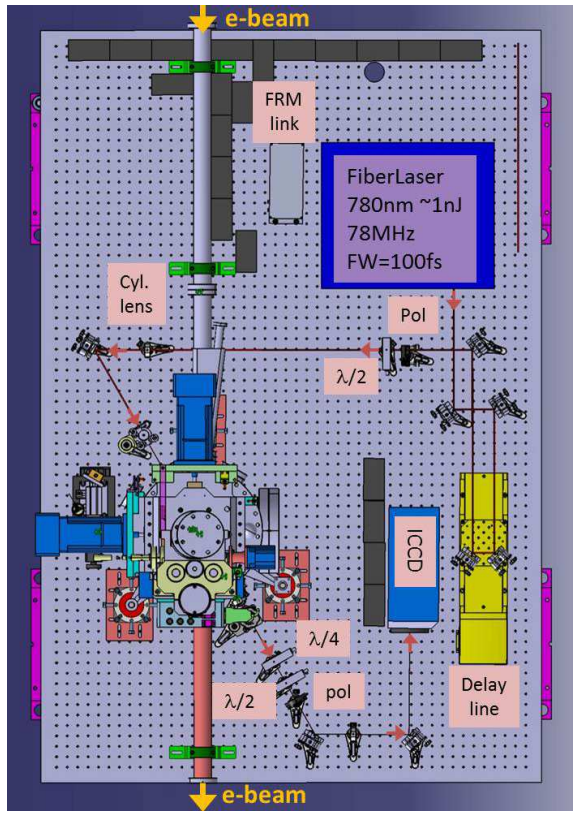

Figure 1: EOS FEL1 layout top view. Electron beam traveling in the beam pipe from top to bottom.

holder. The crystal EO response has been tested using a THz emitter before installing them in EOS diagnostics [8]. The EO crystals have been protected from the seed laser by using 1.5 mm thick fused silica optical substrate with a high reflectivity coating at 260nm placed in front of the EO crystal. The fused silica does not affect the propagation of the 780 nm fiber laser pulses, while we expect a reduction of the effective THz electric field on the EO crystals. THz field reflections are expected only outside the temporal window of measurement. The laser beam propagation direction presents an angle of 30 degree with the normal to the surface of the crystal. This angle is needed to exploit the spatial encoding scheme. The entrance and exit windows are made of fused silica. At the exit of the vacuum chamber the laser passes through the polarization analysis system usually set in cross polarizers configuration. This consists of two zero order waveplates, a $\lambda/4$, followed by a $\lambda/2$ and a finally a Wollaston prism. The majority of the intensity goes to a dump, while the other branch is directed towards intensified gated CCD camera (ICCD) model *Dicam Pro* produced by PCO. The ICCD is used with a gate time of 10 ns to select only the laser pulse in the 78.895 MHz train that has been affected by the electro optical effect induced by the electron beam. Two imaging lenses $l1$ and $l2$ with focal lengths of respectively 200 mm and 400 mm are installed in the air path at the exit of the vacuum chamber. This lens system produces at the

ISBN 978-3-95450-119-9

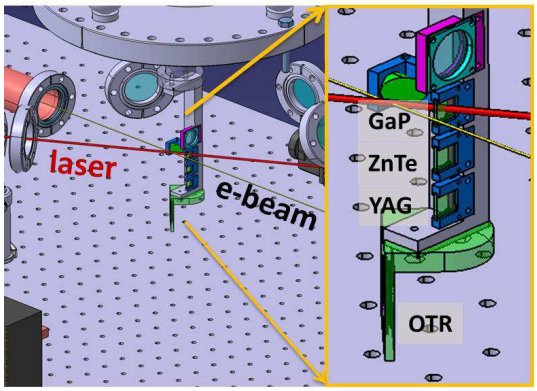

Figure 2: EOS FEL1 crystal holder. From bottom to top: OTR, YAG, ZnTe, GaP, calibration target. Laser and e-beam in red and yellow lines respectively.

ICCD exit image (ICCD included) a final magnification of about 0.5.

TEMPORAL ALIGNMENT

The first temporal alignment is that of the ICCD gate to the laser pulse that modulated at 10Hz. To do this the OTR emitted from the OTR target is steered by Al mirrors onto the ICCD and a tuning of the ICCD trigger delay is done to center the ICCD gate of 10 ns to the OTR signal. Then, a coarse alignment of the EOS laser is performed to about few tens of ps to allow for a short final search of the EOS signal time window alignment with the optical delay line. It is performed with the system depicted in Figure 3. An horizontal translation stage (MICOS ZVT80) and a vertical actuator (Newport NSA12), both motorized and remotely controlled, allow to detect with two different fast photodiodes the EOS laser reflected by the OTR screen and the OTR signal emitted by the OTR screen. The signals are acquired by a Tektronics 6 GHz high bandwidth oscilloscope. The signals are overlapped in time at the EOS chamber center when a specific temporal distance at the oscilloscope is met. This distance is defined on the basis of a measure of geometrical optical paths of the two radiations and of the measured propagation delay induced by the cables (due to length and propagation speed of the signal). After the alignments the remaining uncertainty is about 100 ps. At this point the EO signal is looked for by moving the optical delay line. This systems is also used for coarse temporal alignment diagnostics of the seed laser arrival time to the electron beam arrival time. In the case of coarse alignment of the seed laser, the OTR screen is used both to emit OTR radiation and to reflect the seed laser radiation. Since they are collinear both are directed on the same fast photodiode (modified by removing the protection window which would absorb the seed laser radiation at 260 nm). The photodiode has a small active area of 200 x 200 μm and for this reason it is mounted on a remotely controlled horizontal and vertical translation system. In this case, since only one photodiode is involved, the temporal alignment can be measured with an accuracy better than few picoseconds.

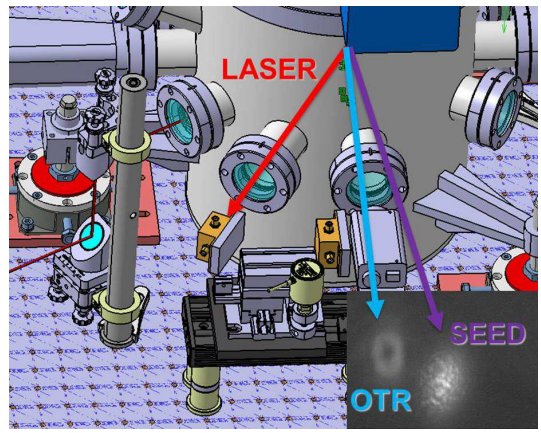

Figure 3: EOS FEL1 coarse temporal alignment system layout.

LONGITUDINAL PROFILE MEASUREMENT

The ICCD time calibration is performed comparing the calibrate spot size of the laser on the crystal as seen with an external camera to the size of the laser on the ICCD. The time windows of the measurement depends on the angle and on the laser transverse spot size at the EO crystal (see Figure 4). The laser spot on the crystal has a FWHM of 3.3 mm corresponding to a time window of 5.6 ps. On the ICCD the laser spot has a FWHM of 350 pixels. With the present setup the calibration factor is of 17 fs/pixel. Measurements have been performed with both ZnTe and

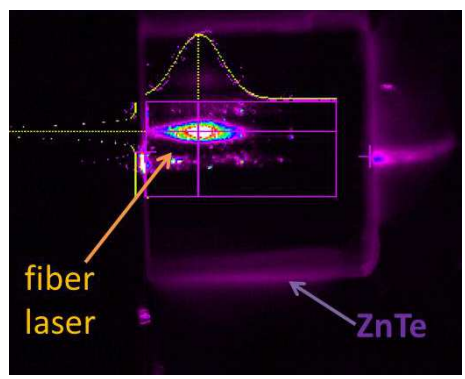

Figure 4: Laser spot on the ZnTe crystal as seen by an external CCD camera.

GaP. In the first case the EO signal is pretty large with good signal to noise ration and negligible background. In the second case the background is not negligible, a background subtraction is needed and the SNR is lower. This effect is expected because the rotation induced in the case of GaP is smaller due to a smaller electro-optic coefficient and smaller thickness. For both crystals, the best SNR is found

ISBN 978-3-95450-119-9

about 3-5 degrees off extinction of the polarizers. The polarization extinction ratio is about 2500 mainly limited by the residual stress of the vacuum windows. The Figure 5 show a EO signal measured with ZnTe 1mm thick crystal for a moderate compression factor (CF). The left graph shows a series of consecutive shot with average bunch duration of 1.5 ps FWHM. For comparison with high compression the image on the right shows bunch profiles with average FWHM of 790 fs. These measurement performed during a phase fluctuations of the plants upstream of the magnetic compressor show the capability of the system to detect the time jitter and the compression factor jitter induced by jitter in the RF plants. For higher compression

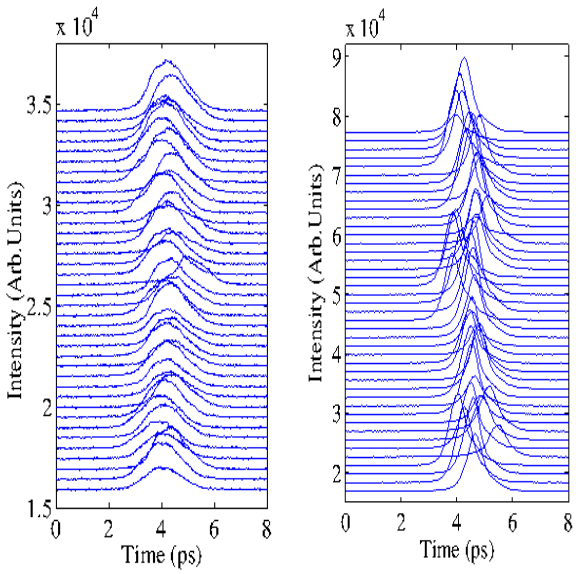

Figure 5: EOS longitudinal profile measurement sequences. With CF=3.5 (left) the average FWHM is 1.5 ps. At CF=8.5 (right) the average FHWM is 790 fs.

factor the crystals chosen for initial operation (ZnTe 1mm and GaP 0.4 mm) are limiting the temporal resolution of the system. We plan the installation of an 0.1 mm GaP crystal together with new entrance and exit windows to improve the polarization extinction ratio.

TIME JITTER MEASUREMENT

By using the EOS on FEL1 a time jitter measurement with good temporal resolution is also possible. As an example we report in Figure 6 a sequence of 50 EOS acquisitions at 1 Hz, acquired during a normal operation of the accelerator with minimal time jitter. The time jitter is measured as shot to shot displacement of the centroid and it is typically of the order of 70 fs rms for a compression with a single bunch compressor to a bunch length FWHM of about 1 ps. This measurement is a direct and single shot measurement of the relative arrival time of the electron bunch with respect to the pulse of the EOS laser, which is phase locked to the optical femtosecond pulsed phase reference, distributed to all the laser systems of FERMI@Elettra. The relative phase jumps (or drifts) are sampled at the bunch repetition rate (10Hz for FERMI) and directly expressed in time units. These measurements, as opposed to the ones based on single side band phase noise analysis, can be directly compared to other systems, like the RF deflecting cavities or the Bunch Arrival Monitor (BAM), also installed on FERMI@Elettra.

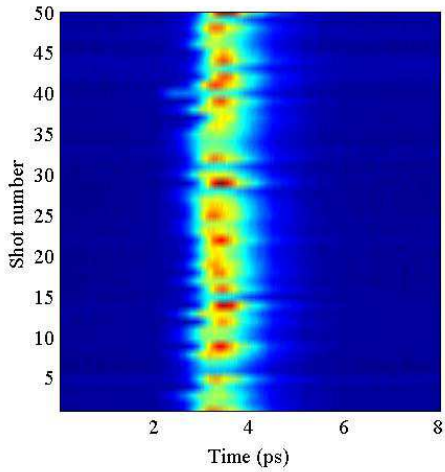

Figure 6: EOS signal intensity map over 50 shots. Time jitter of 70 fs rms. Data acquired using a ZnTe 1 mm thick crystal.

ACKNOWLEDGMENT

The system was initially installed at SPARC (LNF-INFN) then been moved to FERMI@Elettra for it first operation. We would like to thank D. Filippetto, A. Cianci, M. Bellaveglia, G. Gatti, A. Mostacci (INFN-LNF), L.Giannessi and M. Del Franco (ENEA) for their support during SPARC activities and S. Jamison (STFC-Alice), P. Krejcik and D.Fritz (SLAC) for very useful discussions and advice. This work was partially supported by the Italian Ministry of University and Research under grants FIRB-RBAP045JF2 and FIRB-RBAP-6AWK3.

REFERENCES

[1] G. Berden, et al., Phys. Rev. Lett. **93**, 114802 (2004).

[2] G. Berden et al. PRL 99, pg 164801 (2007).

[3] A. Cavalieri et al. PRL 94 pg 114801 (2005).

[4] A. Azima et al. MOPCH011 Procs. EPAC (2006).

[5] J. D. Jackson “Classical Electrodynamics”, 2nd ed., Wiley, Canada (1975).

[6] M.Veronese et al., TUPTPF026, Proc. BIW08, (2008).

[7] M. Ferianis et al., FROAI2, Proc. FEL2011 (2011).

[8] M.Veronese et al., TUPC12, Proc. FEL2009 (2009).

ISBN 978-3-95450-119-9